CHAPTER 6

MISCELLANEOUS PROBLEMS

By Seizo MOTORA

6.1 THE MANOEUVRABILITY OF SHIPS UNDER THE EFFECT OF WIND

6.1.1 Introduction

A very interesting work in this field was done by NAKAJIMA [34] under the instruction of KINOSHITA as summarized in this section.

In Fig. 6.1 a ship is supposed to advance at speed V when she meets a gale of speed U and relative angle φ. Due to the wind pressure, the ship will be acted by the lift L_A and drag D_A which will cause the ship to drift at drifting angle β. By the drifting, the ship hull together with the rudder will create the hydrodynamic lift L, drag D, and moment N until the windward component of the hydrodynamic force balances with the wind drag. At this condition, the total summation of forces including ship's thrust is zero. However, the summation of the moment including moment due to the rudder at maximum helm angle will not necessarily be zero.

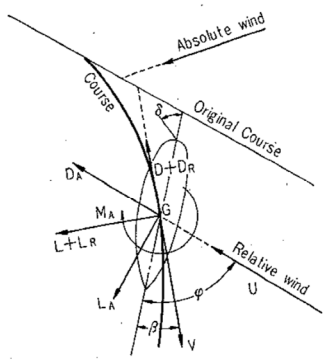

FIG. 6.1 RELATION BETWEEN THE SHIP AND THE WIND

If the summation of the moment is not zero, and is in a direction to increase φ, the ship will have a tendency to turn windward. If the moment is in an inverse direction the ship will turn leeward. In both cases, the ship is supposed to be uncontrollable. If the summation of the moment is zero within the range where rudder angle δ does not exceed 35 degrees, the ship can keep its heading so that she is supposed to be controllable.

6.1.2 Wind Effect on Train Ferries

NAKAJIMA conducted an experiment on train ferries "Toya Maru" and "Kitami Maru" to measure hydrodynamic force and moment L, D and N. Results are as shown in Fig. 6.2 where L_R, D_R and N_R represent the rudder forces and moment. Making use of data of wind drag and lift on ferry boats Toya Maru and Kitami Maru measured by HANAOKA [8],

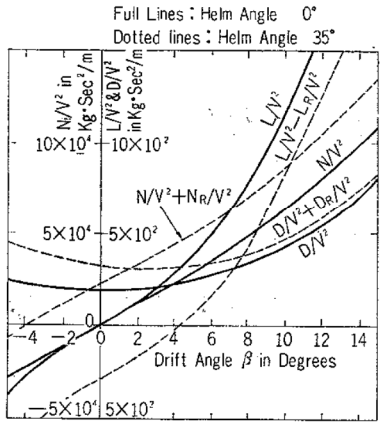

FIG. 6.2 HYDRODYNAMIC FORCE AND MOMENT

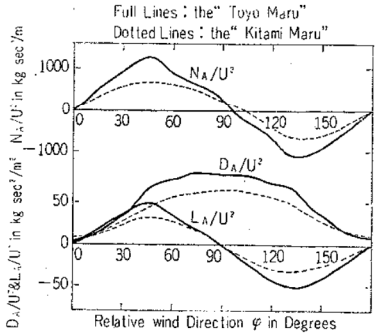

FIG. 6.3 MOMENTS AND FORCES CAUSED BY THE WIND

shown in Fig 6.3, NAKAJIMA made up diagrams by which controllability of those ships are clearly observed. Fig. 6.4 shows the controllability of Toya Maru and Kitami Maru when their rudders are kept amidship. The base of the diagram is the relative wind direction and the ordinate is the ratio of relative wind velocity over ship speed. It is easily seen by Fig. 6.4 that these ships have strong trend to turn windward.

Fig. 6.5 shows the controllability of Toya Maru when her rudder is laid 35 degrees to the direction to cancel the wind moment. The ship is controllable at relatively mild wind compared with ship speed. She becomes to be uncontrollable to turn windward at strong wind, and at very strong wind, she becomes controllable again in a very narrow range. Then she becomes uncontrollable again to turn leeward at very high wind speed and at ahead condition.

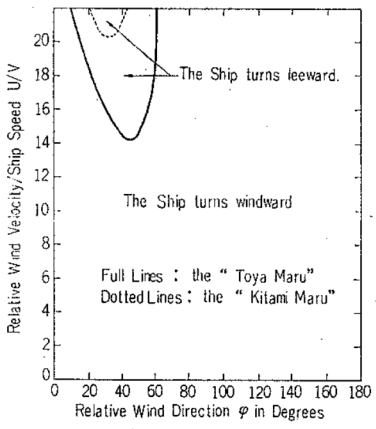

FIG. 6.4 WIND EFFECT ON THE MOTION OF TRAIN FERRIES

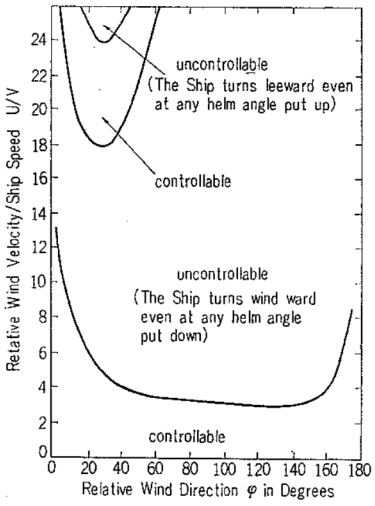

FIG. 6.5 WIND EFFECT ON THE MANOEUVRABILITY OF THE "TOYA MARU"

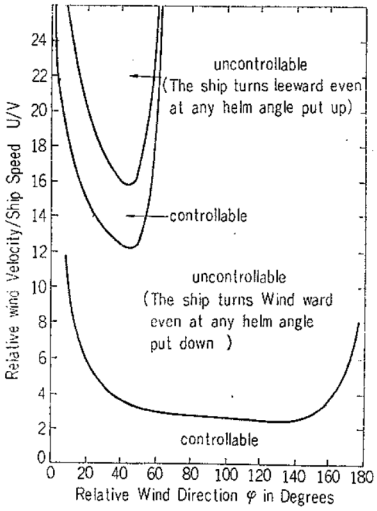

FIG. 6.6 WIND EFFECT ON THE MANOEUVRABILITY OF THE "KITAMI MARU"

Fig. 6.6 is the same diagram on Kitami Maru which has smaller superstructure than Toya Maru.

6.1.3 Wind Effect on Fishing Boats

The same analysis was made on fishing boats Shin-Nihon Maru No. 5 and Seishu Maru No. 7. Special reference was made on the effect of spanker and trim. Fig. 6.7 to Fig. 6.9 show the effect of trim. From these figures it is easily seen that the ship inevitably turns to the windward at trim by the bow condition, and that the ship is more controllable at even keel, and that the ship inevitably turns leeward until she becomes abeam condition. Fig. 6.10 and Fig. 6.11 show the effect of spanker. It will be noticed that the controllability is improved by the effect of spanker.

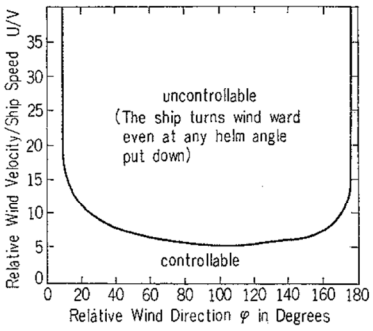

FIG. 6.7 WIND EFFECT ON THE MANOEUVRABILITY OF THE "SHIN-NIHON MARU NO. 5" IN THE CONDITION OF TRIM BY THE BOW

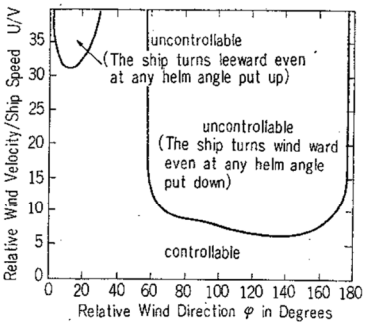

FIG. 6.8 WIND EFFECT ON THE MANOEUVRABILITY OF THE "SHIN-NIHON MARU NO. 5" IN THE CONDITION OF EVEN KEEL

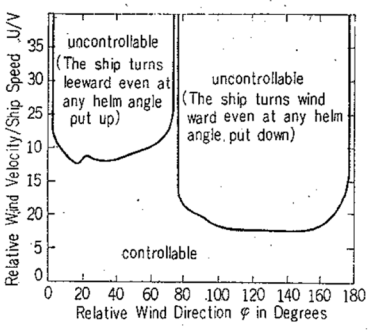

FIG. 6.9 WIND EFFECT ON THE MANOEUVRABILITY OF THE "SHIN-NIHON MARU NO. 5" IN THE CONDITION OF TRIM BY THE STERN

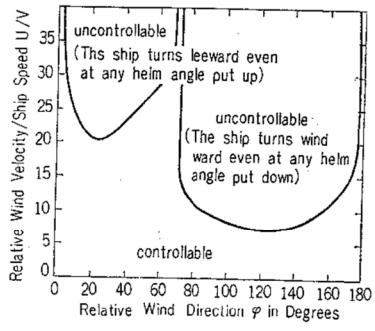

FIG. 6.10 WIND EFFECT ON THE MANOEUVRABILITY OF THE "SHIN-NIHON MARU NO. 5" IN THE CONDITION OF EVEN KEEL WITHOUT SPANKER

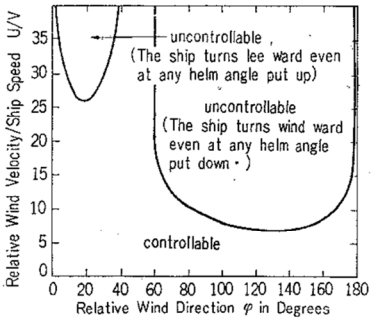

FIG. 6.11 WIND EFFECT ON THE MANOEUVRABILITY OF THE "SEISHU MARU NO. 7" IN THE CONDITION OF EVEN KEEL

6.2 KINEMATIC CONSIDERATIONS ON THE EFFECTIVENESS OF A BOW-THRUSTER

—Special reference to the influence of its location and ship speed—

6.2.1 Introduction

When a ship is at rest or at very low speed, a bow-thruster is much effective to turn the ship. But it is well known that the effectiveness decreases rapidly as the ship speed increases. The following two reasons are to be supposed to explain this phenomenon.

(1) possible decrease of the side thrust derived from a bow thruster as the ship speed increases.

(2) remarkable decrease of turnability of a ship from the kinematic reason.

MOTORA and FUJINO [32] have treated this problem, making special reference to the kinematic consideration as is summarized in this section.

6.2.2 Effect of Location of a Bow-Thruster

In a case where the drift angle β and the turning angular velocity r are very small compared with the ship speed, the equation of motion can be expressed as follows:

$$\left.\begin{aligned} -(m'+m_y')\dot{\beta}' &= Y_\beta'\cdot\beta' + \{-(m'+m_x')+Y_r'\}r' + Y_\delta'\delta' + Y_b' \\ (I_z'+J_z')\dot{r}' &= N_\beta'\cdot\beta' + N_r'\cdot r' + N_\delta'\cdot\delta' + N_b' \end{aligned}\right\} \quad (6.1)$$

where, Y is the hydrodynamic side force.
N is the hydrodynamic moment about z axis.
δ is the rudder angle.
Y_b is the side thrust derived from a bow-thruster.
N_b is the moment due to the side-thrust.

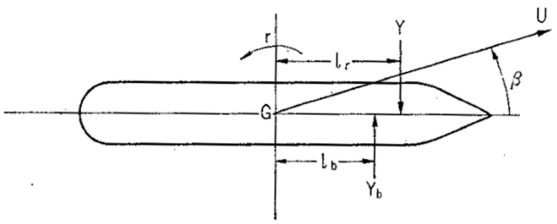

FIG. 6.12

Supposing a ship advancing on a straight course until the prescribed instant ($t>0$) and being imposed a side force Y_b and moment N_b at $t=0$, the angular velocity r of the ship is given as follows; (in this case, the rudder remains amidship)

$$r' = \frac{Y_\beta' N_b' - N_\beta' Y_b'}{C'}\{1+f(t)\} \quad (6.2)$$

where, C' is the discriminant of ship's directional stability, i.e.

$$C'=\{-(m'+m_x')+Y_r'\}N_\beta'-Y_\beta'N_r' \tag{6.3}$$

In equation (6.2), a time function $f(t)$ does not depend on the amount of the side force Y_b, but on both the location of Y_b and the ship's steering characteristics itself, and is expressed as the sum of two exponential functions which become rapidly zero as the time passes. Therefore, the angular velocity r approaches rapidly to a stationary value r_s', which is given as follows, by taking into account $N_b'=Y_b'l_b'$ and $N_\beta'=Y_\beta'l_r'$,

$$r_s'=\frac{Y_b'Y_\beta'}{C'}(l_b'-l_r') \tag{6.4}$$

where $l_r'=l_r/l$, $l_b'=l_b/l$.

Since l_b-l_r is the distance between the point of application of the side thrust Y_b and that of the hydrodynamic force Y, it will be easily seen that the side thrust Y_b gives the ship a moment with moment lever of l_b-l_r. According to the above statement,

(1) In the case where the side force Y_b is located ahead of the hydrodynamic force Y, the bow of the ship turns to the direction of Y_b as is intended. (To be called as "ordinary turning".)

(2) In the inverse case, that is, the side force Y_b is located abaft the hydrodynamic force Y, the bow of the ship turns to the counter direction. ("inverse turning")

However, when a ship is at rest, she turns to the ordinary direction even in the latter case. It should be noted that the above statement is valid for the stationary condition. In the latter case, just after the side thrust is applied, the ship turns to the ordinary direction, then gradually changes its turning direction as the time passes as shown in Fig. 6.13. In Fig. 6.13, the features of the angular velocity r are shown on a time basis in various cases of location of the side thrust Y_b calculated for Series 60, $C_b=0.60$ ship.

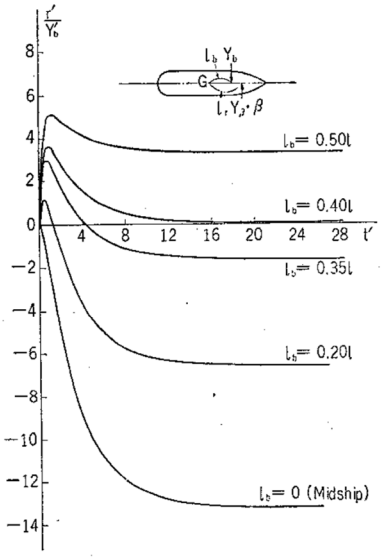

FIG. 6.13 INFLUENCE OF THE LOCATION OF A BOW-THRUSTER

6.2.3 Effect of the Speed of Advance

Next, we will consider the influence of advance speed. In the case of no advance speed, since the hydrodynamic force and turning moment which come from the presence of drift angle β are not generated, the re-

sultant turning moment is given as a product of the side force Y_b by the distance between its application point and the C. G. of the ship. Therefore, the ship's bow always turns to the direction of Y_b and the turning angular velocity r is expressed approximately as follows;

$$r'=\sqrt{\frac{-N'_b}{N'_{rr}}}\tanh\left(\sqrt{\frac{-N'_{rr}N'_b}{I'_z+J'_z}}t'\right) \tag{6.5}$$

where the coefficient N'_{rr} means the coefficient of the velocity squared damping moment against turning motion. When the advance speed is very small, the equation of motion is essentially non-linear, but as the speed becomes larger compared with the angular velocity r, the equation of motion is represented by such a linear equation as Eq. (6.1).

In cases of different advance speed, the angular velocity r is calculated for the case $l_b=0.35l$ and shown in Fig. 6.14. In Fig. 6.15, the same results are re-plotted, with the time interval as a parameter.

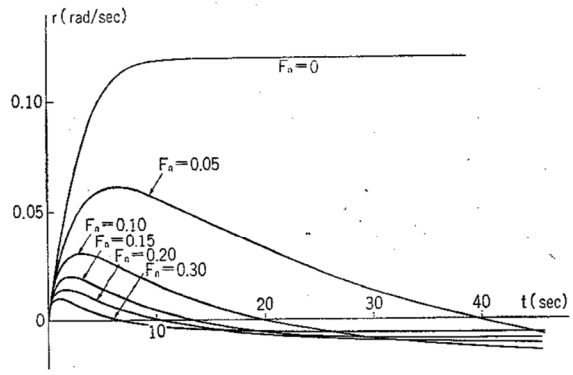

FIG. 6.14 INFLUENCE OF SHIP SPEED

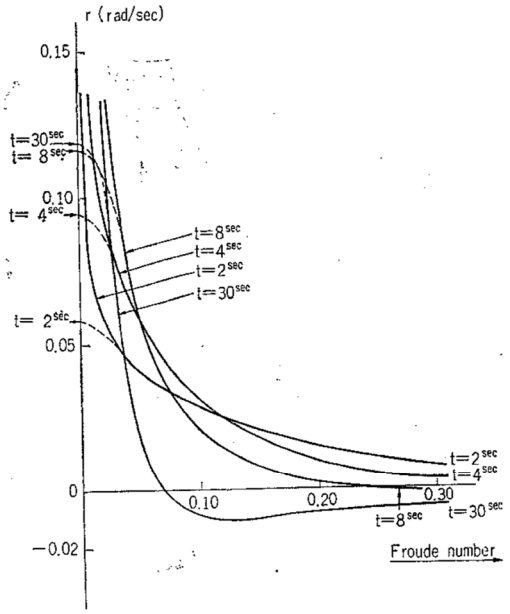

FIG. 6.15 INFLUENCE OF SHIP SPEED (WITH THE TIME INTERVAL AS A PARAMETER)

From these figures, it can be concluded that the effectiveness of a bow-thruster decreases rapidly at around Froude number=0.06. Fig. 6.16 is the full scale trial data on M. S. Tansei Maru. A remarkable decrease of the effectiveness of the bow-thruster due to advance speed will be recognized. However, in this case, since the location of the bow-thruster was ahead of the hydrodynamic force Y, the ship did not turn inversely.

In summarizing, the following can be concluded:

a) If a ship is at rest, the effectiveness of a bow-thruster is propor-

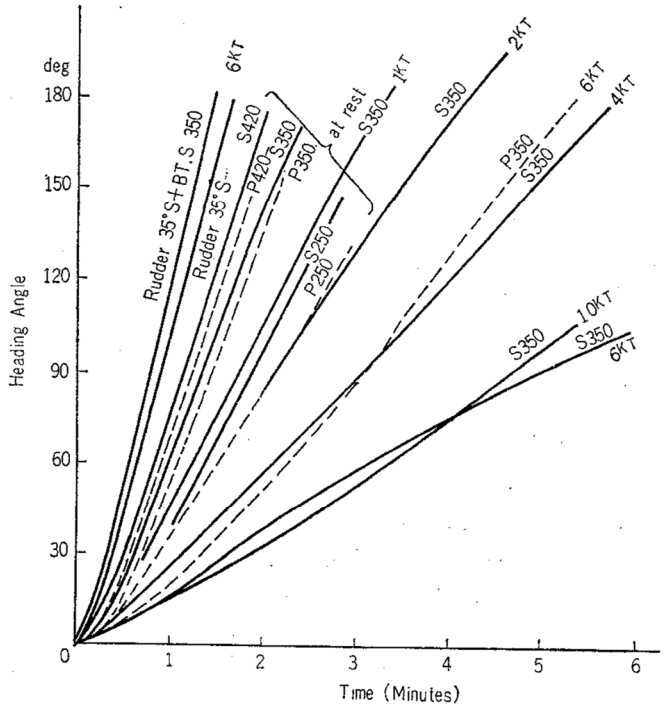

FIG. 6.16 EFFECTIVENESS OF A BOW THRUSTER AT REST AND WITH ADVANCE SPEED

tional to the distance between the C. G. of the ship and the location of the thruster (l_b).

b) If a ship has speed of advance, the effectiveness of a bow-thruster decreases rapidly as the time passes because of the change of moment lever from l_b to $l_b - l_r$.

c) In the case where $l_b - l_r$ is negative, i.e. the bow-thruster is located abaft the location of hydrodynamic side force Y, a ship will finally turn to the inverse direction as the time passes.

6.3 AN IMPROVEMENT OF SHIP'S STEERING QUALITIES BY MEANS OF AUTOMATIC CONTROL

6.3.1 Relation between the Course Keeping Qualities and the Turning Qualities of Ships

It is well known that the course keeping quality and the turning quality of a ship are contradictory to each other, and that it is impossible to improve both of them without increasing rudder area. This relation will well be explained by Fig. 6.17 where the base is inverse of NOMOTO's T value [37] which is related to the course keeping quality and the ordinate is inverse of NOMOTO's K value which is related to the turning ability.

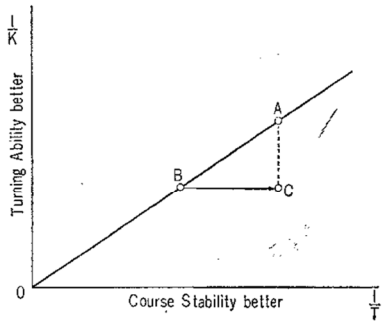

FIG. 6.17 RELATION BETWEEN TURNING ABILITY AND COURSE STABILITY

In Fig. 6.17, supposing that a ship B has a poor course keeping quality, a trial is made to improve the ship's course keeping quality by changing ship form and stern profile. This trial will result in the decline of the turning ability as well as the improvement of course keeping quality and ratio K/T remains almost unchanged. This change is indicated in Fig. 6.16 by the shifting of the ship B to the ship A.

MOTORA and KOYAMA [33] tried to make use of automatic control which is superposed upon the manual control to improve ship's steering quality. They showed that a ship B which has an arbitrary steering quality can be automatically controlled so that she behaves as if she has the same steering quality as a specified ship A has.

Supposing the ship B has poorer course keeping quality than the ship A has, by virtue of the automatic control the ship B will behave as if she is more stable than it was.

Since a ship with poor course keeping quality such as the ship B has better turning ability, it is possible for ship B to turn quickly if the automatic control is shut off. Therefore, the ship B with control will have the course keeping quality as the ship A has, and naturally has the turning ability as it is when the automatic control is shut off. This means that the ship can behave as a ship C shown in Fig. 6.17.

6.3.2 Conditions of Automatic Control

A linear equation of motion of a steered ship is shown as equation (6.6) where $a_1 \sim a_4$ and c_1, c_2 are coefficients.

$$\ddot{r}' + 2a_1\dot{r}' + a_2 r' = c_1\dot{\delta}' + (a_4 c_1 + a_3 c_2)\delta' \tag{6.6}$$

If the rudder angle δ' is controlled automatically proportional to the angular velocity r' and the angular acceleration $\dot{r}'$, the δ' in equation (6.6) becomes as follows:

$$\delta' = -\sigma_1 r' - \sigma_2 \dot{r}' + \sigma_3 \delta'^* \tag{6.7}$$

where δ'^* is the rudder angle given by the manual control σ_1, σ_2 and σ_3 are the intensities of control.

Substituting (6.7) into (6.6) we get:

$$\begin{aligned}\ddot{r}' + 2a_1\dot{r}' + a_2 r' = {} & c_1(-\sigma_1\dot{r}' - \sigma_2\ddot{r}' + \sigma_3\dot{\delta}'^*) \\ & + (a_4 c_1 + a_3 c_2)(-\sigma_1 r' - \sigma_2\dot{r}' + \sigma_3\delta'^*)\end{aligned} \tag{6.8}$$

Since there are three parameters σ_1, σ_2 and σ_3 to be chosen arbitrarily, we can change three coefficients out of four coefficients of the equation (6.8). Therefore, it will then be possible to bring the steering quality of a ship to be almost equal to that of other ship, letting just one coefficient (say the coefficient of δ') to be unequal.

6.3.3 Numerical Example

Let us consider a Series 60, $C_b=0.60$ model as a standard ship (ship A) which is supposed to have a satisfactory course stability. Then let us consider ships B, C, D and E which have poorer course stability than the ship A. These ships are supposed to have identically the same derivatives the ship A has except N_β.

The stability indices of these ships are as follows.

ship	A	B	C	D	E
a_2	1.029	0.5146	0	−0.5146	−0.7683

The intensities of control σ_1, σ_2 and σ_3 which are necessary to make the manoeuvrability of ships B, C, D and E equal to that of ship A, are shown in Fig. 6.18. It should be mentioned that the increment of the manipulated values does not become too large as the intensity of instability of ship increases. To examine how close the manoeuvrabilities of ships B, C, D and E with control are to that of ship A, inditial responses of these ships are calculated.

The responses of uncontrolled ships are as shown in Fig. 6.19, while the responses of controlled ships are as shown in Fig. 6.20. Fig. 6.21 shows the rudder angles which are required by the automatic control. From

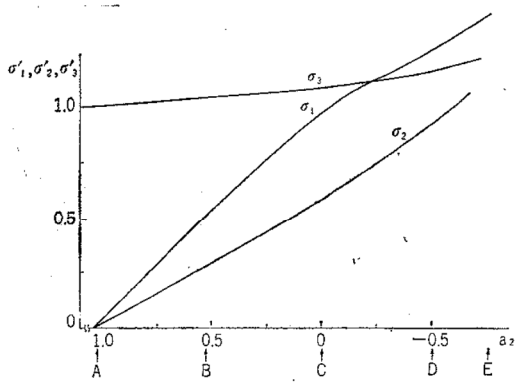

FIG. 6.18 VALUES OF σ'_1, σ'_2 AND σ'_3 TO GIVE AN EQUIVALENT MANOEUVRABILITY AS THE SHIP A

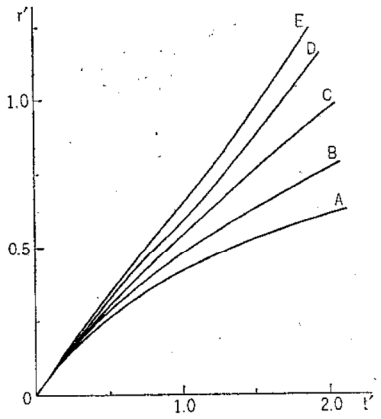

FIG. 6.19 INDITIAL RESPONSES WITHOUT THE AUTOMATIC CONTROL

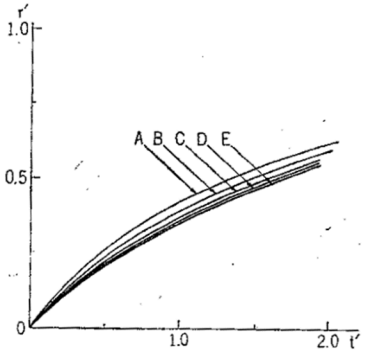

FIG. 6.20 INDITIAL RESPONSES WITH THE AUTOMATIC CONTROL

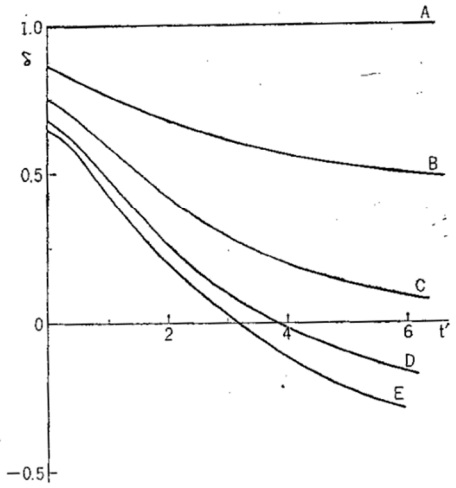

FIG. 6.21 RUDDER ANGLES REQUIRED BY THE AUTOMATIC CONTROL

these examples, it can be said that it is possible to convert the manoeuvrability of a ship to be almost equal to that of any other ship.

6.4 MANOEUVRABILITY IN CONFINED WATERS

This problem has long been subject to interests of naval architects, and many works have been done in this field all over the world. Two remarkable approaches have also been done in this field in Japan in recent years.

6.4.1 Turning Tests in Shallow Water

KOSEKI, YAMANOUCHI, MATSUOKA and YAMAZAKI [21] have jointly conducted model experiments in shallow water using 4.50 meter models of a super tanker Nissho Maru and a cargo ship. Particulars of both models are as given in Table 6.1. Fig. 6.22 shows the spiral test results of the cargo ship where the base is the helm angle and the ordinate is the non-dimensional angular velocity $r=\dot{\phi}L/V$. Fig. 6.23 is also the spiral test data of the super tanker where the rudder-area ratio was changed from 1/60 to 1/80 to check the effect of the rudder area. To examine the effect of water depth upon the turning angular velocity, the ratio r_H/r_∞ in percentage is plotted against the depth ratio H/d as showh in Fig. 6.24 where r_H is the angular velocity at the water depth H, and r_∞ is the angular velocity at the water depth infinity.

From Fig. 6.24, it can be easily seen that the shallow water effect is practically negligible when the water depth is $3.7d$ or more, and that the shallow water effect increases rapidly when the water depth becomes less

TABLE 6.1 PRINCIPAL DIMENSIONS OF SHIP MODELS, RUDDERS AND PROPELLERS

Models	Cargo ship	Super tanker (Nissho Maru)
Length between perpendicular (L)	4.500 m	4.500 m
Breadth (B)	0.6166 m	0.7021 m
Full load draft (d)	0.2466 m	0.2695 m
L/B ratio	7.30	6.41
B/d ratio	2.50	2.61
Block coefficients (C_b)	0.70	0.81
Rudder		
Rudder type	Balanced-Rudder	Balanced-Rudder
Rudder height (h)	176.4 mm	159.1 mm
Rudder length (l)	104.8 mm	113.3 mm
Maximum thickness (t)	18.9 mm	17.9 mm
Aspect ratio (h/l)	1.68	1.40
Maximum thickness to length ratio (t/l)	0.180	0.158
Propeller		
Diameter	180.0 mm	120.6 mm
Boss ratio	0.250	0.189
Pitch ratio (constant)	0.80	0.730
Expanded area ratio	0.40	0.575
Maximum blade width ratio	0.242	0.223
Blade thickness ratio	0.045	0.0635
Rake	10°-18′	9°-58′
Blade number	4	5
Direction of turning	right	right

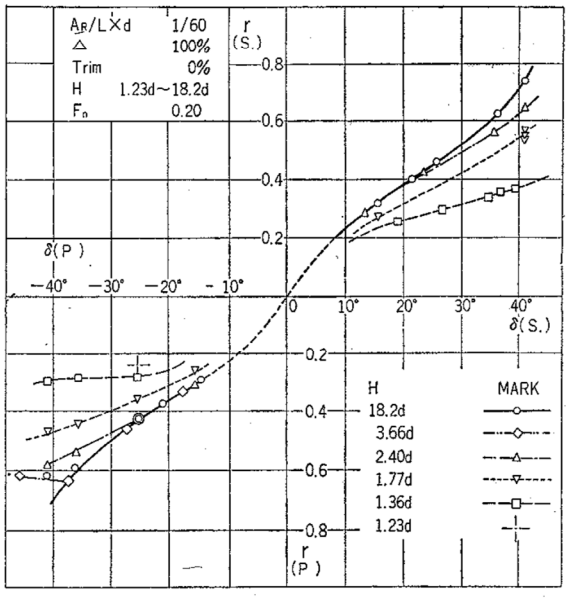

FIG. 6.22 r-δ CURVE OF CARGO SHIP

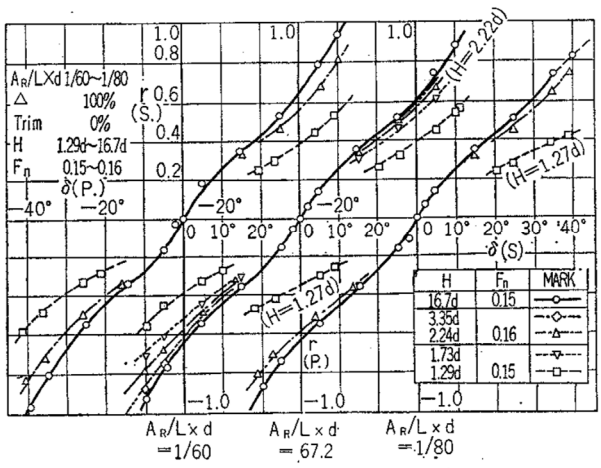

FIG. 6.23 r-δ CURVE OF NISSHO MARU

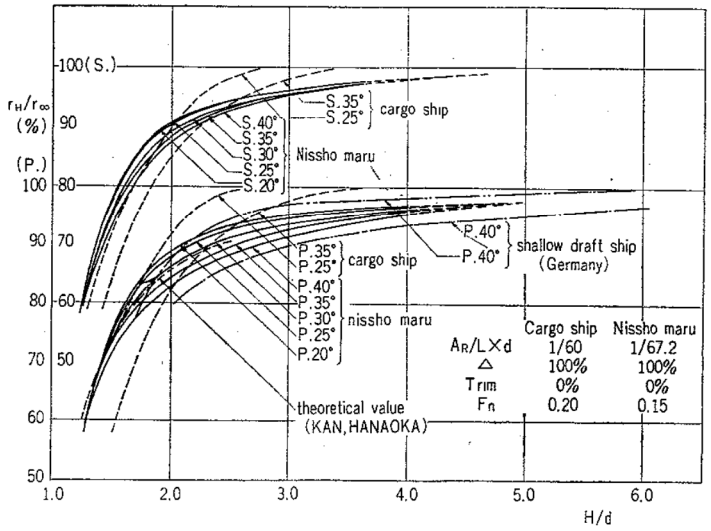

FIG. 6.24 REDUCTION OF r DUE TO LIMITED WATER DEPTH

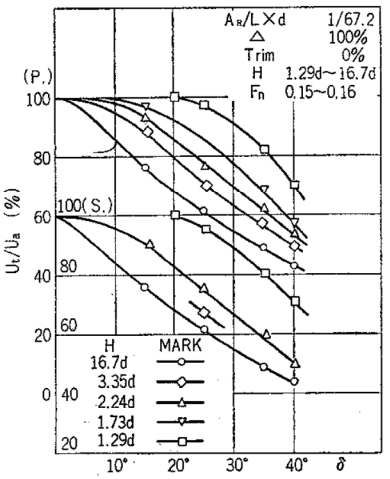

FIG. 6.25 SPEED REDUCTION OF NISSHO MARU

than $2.3d$. This feature agrees with a full scale spiral test data conducted by MOTORA and COUCH [30].

Speed reduction at turning is as shown in Fig. 6.25 where one will easily be aware of an interesting fact that the speed reduction decreases in shallow water.

6.4.2 Theoretical Analysis

Theoretical approach has been also done by KAN and HANAOKA [18] making use of low aspect-ratio wing theory. They treated a thin ship moving at speed V with drifting angle β.

Assuming the boundary condition of the free surface approximately equal to that of rigid boundary, the flow field around the ship can be replaced by the flow field around bodies of breadth $2d$ equally spaced $2H$ on z axis with uniform flow at the speed of $V\beta$ from y direction.

(1) *Shallow water effect on the normal force*

Integrating pressure on the ship's surface, the ratio of the normal force at the water depth H to that at the water depth infinity is obtained as follows.

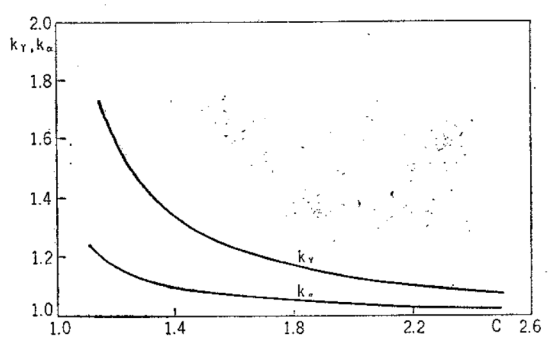

FIG. 6.26 CURVES OF k_Y, k_α

$$\frac{Y_{\beta H}}{Y_{\beta\infty}} = \frac{4c}{\pi^2}\int_{-1}^{1} \cosh^{-1}\frac{\cos(\pi b/2c)}{\cos(\pi/2c)}\,db = k_Y \tag{6.9}$$

where, $c=H/d$ and $b=z/d$

k_Y is shown in Fig. 6.26 on H/d basis.

(2) *Shallow water effect on the moment*

The hydrodynamic moment is also obtained by integrating the pressure on the ship's surface, and it will be easily obtained that the effect of shallow water on the moment is exactly the same as that of normal force. viz:

$$\frac{N_{\beta H}}{N_{\beta\infty}}=k_Y \tag{6.10}$$

(3) *Shallow water effect on the rotatory force and moment*

Similar calculation on the rotatory force and moment indicates that the shallow water effect is the same as the previous case.

$$\frac{Y_{rH}}{Y_{r\infty}}=\frac{N_{rH}}{N_{r\infty}}=k_Y \tag{6.11}$$

It will be interesting to note that k_Y is equal to the ratio of the added mass of a flat plate at water depth H and at water depth infinity.

(4) *Shallow water effect on the rudder force*

Effect of shallow water on a rudder of the aspect ratio λ and the attack angle α is given as follows.

$$k_\alpha=\frac{C_{LH}}{C_{L\infty}}=\frac{1+2k(1+\tau)/\lambda}{1+2k(1+\tau-\sigma)/\lambda} \tag{6.12}$$

Where the factors, τ and σ, mean the definitions, given by DURAND [A-8] and k is defined by the relation $C_L=2\pi ki$, i being the effective angle of incidence. k_α is shown in Fig. 6.26 on H/d basis.

(5) *Shallow water effect on the turning rate and the drift angle*

Making use of k_Y and k_α together with the equation of motion of a turning ship, the ratio of turning rate and the drift angle will be obtained as follows:

$$k_r=\frac{r_H}{r_\infty}=k_\alpha\frac{N'_rY'_\beta-N'_\beta Y'_r+(m'+m'_x)N'_\beta}{k_Y(N'_rY'_\beta-N'_\beta Y'_r)+(m'+m'_x)N'_\beta} \tag{6.13}$$

$$k_\beta=\frac{\beta_H}{\beta_\infty}=\frac{k_r}{k_Y}\cdot\frac{k_Y(N'_\delta Y'_r-Y'_\delta N'_r)-(m'+m'_x)N'_\delta}{N'_\delta Y'_r-Y'_\delta N'_r-(m'+m'_x)N'_\delta} \tag{6.14}$$

(6) *Numerical examples*

k_r and k_β are calculated on a Series 60 $C_b=0.60$ model. Results are as shown in Fig. 6.27 where model experiment data by KOSEKI and TSUJI [22] are shown for comparison. In Fig. 6.28, the ratio $Y_{\beta H}/Y_{\beta\infty}$ and $N_{\beta H}/N_{\beta\infty}$

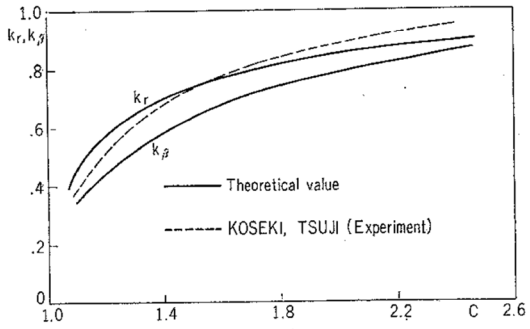

FIG. 6.27 CURVES OF k_r, k_β

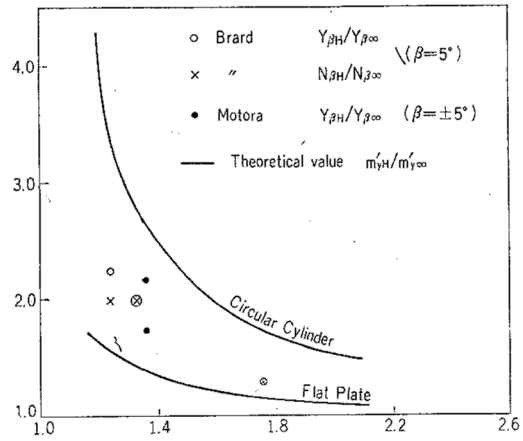

FIG. 6.28 CURVES OF $Y_{\beta H}/Y_{\beta\infty}$

obtained by BRARD [A-4], and MOTORA and COUCH [30] are compared with the added mass ratio of a flat plate and a circular cylinder. From Fig. 6.28, experimental data seem to show reasonable values.